

Modeling of the Compaction Response of Jute Fabrics in Liquid Composite Molding Processes

Gastón Francucci, Exequiel S. Rodríguez

Composite Materials Group (CoMP), Research Institute of Material Science and Technology (INTEMA-CONICET), Materials Engineering Department, Engineering College, National University of Mar del Plata, J. B. Justo 4302, B7608FDQ Mar del Plata, Argentina

Received 18 January 2011; accepted 25 August 2011

DOI 10.1002/app.35543

Published online 6 December 2011 in Wiley Online Library (wileyonlinelibrary.com).

ABSTRACT: In this work, the experimental data of the compaction behavior of jute woven fabrics obtained in a previous work were modeled. A brief description of the current theoretical models found in literature is presented. It was concluded that these theoretical models cannot be used on natural fiber fabrics due to the vast differences in fiber structure and fibers assembly among natural and synthetic fibers. Therefore, two empirical models commonly seen in literature were used to fit the experimental data: the power law and the exponential function. In addition, a novel model was proposed, which represented much better the compaction behavior

of the fabrics. The stress relaxation was also modeled using three empirical models: a power law, a first-order exponential function, and a second-order exponential function. The two-parameter power law model fitted the relaxation curve as well as the five-parameter exponential function. On the other hand, the first-order exponential function could not represent properly the relaxation stage. © 2011 Wiley Periodicals, Inc. *J Appl Polym Sci* 124: 4789–4798, 2012

Key words: biofibers; reinforcement; resin transfer molding; compression; modeling

INTRODUCTION

Nowadays, most manufacturing techniques can be simulated with advanced computer software. This leads to a significant reduction of the manufacture costs by decreasing the amount of experimental determinations of the processing variables, which often involves a trial-and-error process. Thus, materials waste and operational time are minimized prior to obtain a high quality composite part. This computer programs need mathematical models that relate the processing variables with the material properties or behavior. Some models can be developed theoretically, through several assumptions about the material behavior, boundary conditions, and geometric simplifications. These models reduce the total amount of experimental work, even though they must be validated experimentally. On the other hand, empirical models require larger experimental

work, and they are based on fitting the experimental data to obtain analytical relationships between the processing variables and the material properties.

In some liquid composite molding (LCM) processes such as resin transfer molding, the preform (a stack of several layers of the fabric used as reinforcement) is compacted between two rigid mold faces, so its compaction behavior determines the clamping forces required to achieve the desired part thickness, or fiber volume fraction. In other processes such as vacuum infusion, in which one of the mold faces is a flexible plastic film, the compaction force is limited by the atmospheric pressure, and thus the compaction response of the preform determines the maximum fiber volume fraction or the minimum part thickness that can be achieved.¹

During the processing by LCM of composite materials subsequent compressive loading cycles are expected to take place. In some cases where the mold geometry is complex and the lay out of the stack of fabrics is difficult, a preforming step is carried out in order to obtain a preform with shape and thickness close to those of the final part. A binder is sometimes used to avoid preform deformation during handling. Therefore, a complete characterization of fibrous reinforcement should study the compaction response of the first and subsequent loading cycles. In general, the differences between the first and second cycles are significant and between the

Correspondence to: E. S. Rodríguez (erodriguez@intema.gov.ar).

Contract grant sponsor: National Research Council of Argentina (CONICET); contract grant number: PIP 0014.

Contract grant sponsor: SECYT; contract grant number: PICT08 1628.

Contract grant sponsor: National University of Mar del Plata.

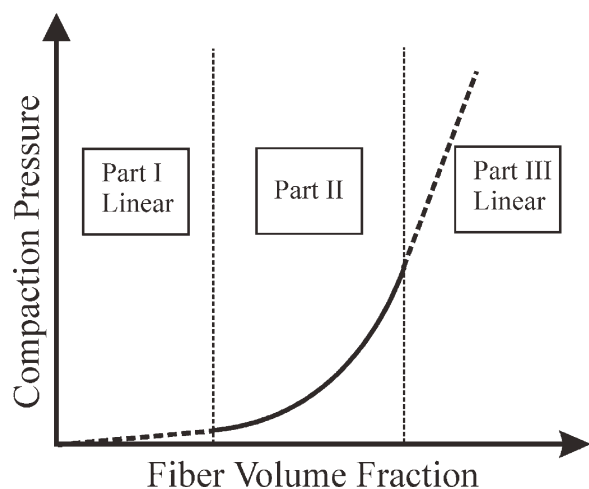


Figure 1 Typical compaction curve of woven fabrics

second and third cycles are small but observable; and after the third cycle no more differences can be distinguished.³

Natural fiber fabrics are becoming a very attractive alternative to synthetic fiber reinforcements to manufacture composite parts in nonstructural applications, due to its low cost and renewable and ecological nature. However, plant fibers' structure and chemical composition are very different than that of synthetic fibers, which affect the processing of these materials. It was found in previous work that both unsaturated and saturated permeabilities of natural fiber fabrics are reduced due to fluid absorption and fiber swelling.² In the same way, it was found in another publication,³ in accordance with other authors,^{4,5} that fiber softening and hollow structure affect the compaction response by reducing the compaction pressure and increasing the permanent deformation of the preforms. Fiber swelling caused by fluid absorption changes the fiber dimensions and

surface roughness, which in turn affects the inter-fiber friction and therefore the compaction behavior of the fabrics. However, the relationship between fiber swelling and interfiber friction has not been studied yet, and it would be a very interesting research topic for further works in this field of study. Because of natural fibers' chemical composition rich in cellulose and hemicellulose, fluid absorption, and, therefore, fiber swelling and softening are more significant when polar fluids are used. If non-polar fluids are used, fibers will absorb less amount of fluid and the softening effect will not be significant. However, it was found in previous investigations² that jute fibers absorbed a small extent (6%) of vinyl ester resin and swelled as a consequence. These differences observed in the behavior of natural fibers when different fluids are used should be taken into account when fabrics' characterization is performed in laboratory experiments that are carried out with a test fluid different from the resin that will be used in real processing conditions. In addition, Umer et al.⁶ studied the effect of yarn length and diameter on the permeability and compaction response of flax fiber mats. Regarding the compaction behavior of these reinforcements, they found that large yarn diameter mats are the least stiff, than medium and small yarn diameter mats and that the large and medium yarn diameter fiber mats showed a moderate fiber lubrication effect under saturated compaction, while almost no lubrication effect was noted for the small yarn diameter mats. They also found that long yarn length mats required larger forces to compact due to the greater number of crossover points between the yarns.

To our knowledge, the modeling of the compaction behavior of natural fiber fabrics has not been studied in literature. In this work, the applicability of current theoretical and empirical compaction

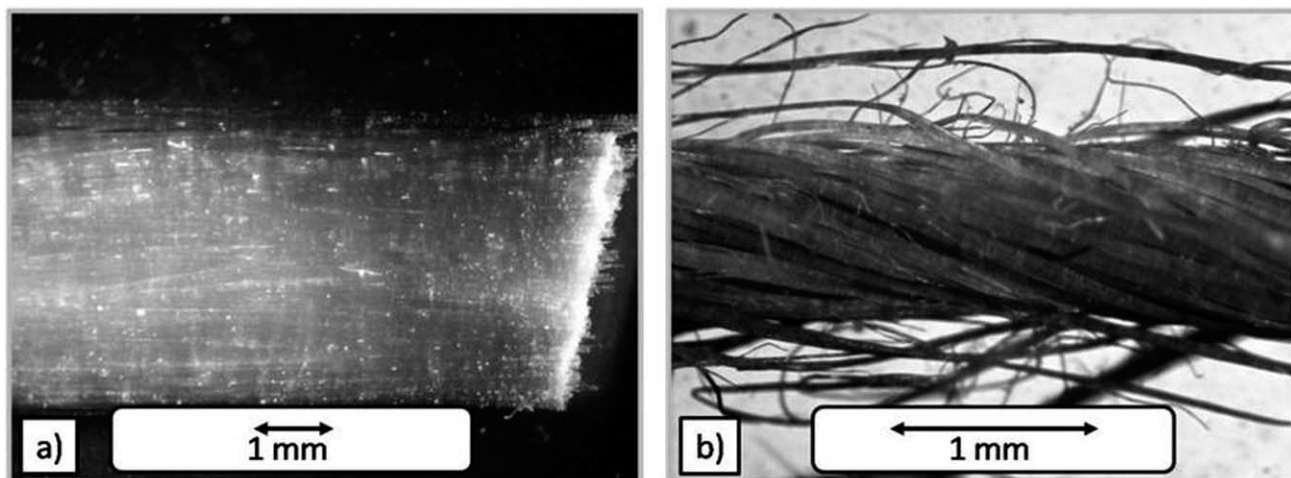


Figure 2 Fiber bundles that compose a woven fabric. (a) A roving of continuous and parallel glass fibers. (b) A yarn of twisted and discontinuous jute fibers

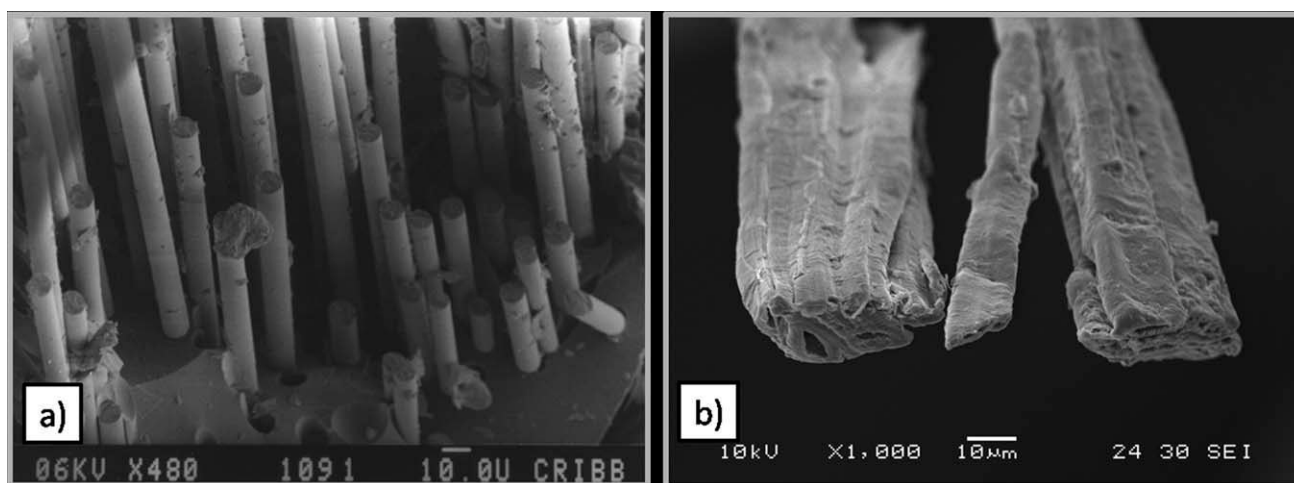


Figure 3 (a) SEM image of glass fibers obtained from a fracture surface of a polymeric matrix-glass fiber composite.²⁰ (b) SEM image of a jute technical fiber showing the bundle of elementary fibers

models on natural fiber fabrics is discussed. In addition, jute woven fabrics' compaction and relaxation processes are modeled based on experimental data obtained in previous investigations.³

THEORY

In general, the pressure–thickness curve for woven fabrics can be divided into three parts, as shown in Figure 1. The first linear part of the curve is related with the reduction of pores and gaps among the fibers,⁷ and the bending of the yarns at low pressures.⁸ In this stage, the resistance of the yarns to compaction is very low, and the curve slope is almost zero. In the second part of the curve, the compressive force increases rapidly, because the reduction in thickness generates an increase in the fiber to fiber contacts and interfiber friction.⁸ In addition, processes such as nesting and shifting between adjacent layers happen in this compaction stage. At the third part of the curve, the voids between fibers are reduced and the slipping of fibers ceases, and thus the linear compaction response is related to the transverse modulus of the fiber itself.⁸

The modeling of the compaction stage in LCM is important to obtain analytical expressions, which relate the fiber volume fraction with the compaction pressure, as the processing variables (compaction speed, number of loading cycles, etc.) are modified. Many authors proposed suitable models to describe the compaction behavior of fiber assemblies.^{8,9–18} Theoretical models are based on many geometric assumptions, material idealizations, and suppositions about the interaction between fibers and tows. Thus, the experimental study of the compaction behavior of the fabrics should always be done to prove the model validity. Chen and Chou¹¹ defined

a unit cell that was considered to be repeated in the plane of the fabric, reducing all the analysis to a small portion of the fabric. They treated the yarn as a beam and as a transversely isotropic solid, assuming that the fibers in the yarn are highly compacted and no voids and gaps exist between the yarns. In addition, they took into account only the elastic deformation, which was considered to take place in the thickness direction. In addition, they hypothesized that during the compaction process, the yarn deforms but its cross-sectional area remains unchanged. In another publication, Chen et al.¹⁰ used the assumptions of microhomogeneity and microisotropy, which imply that the constituent material, that is the solid fiber, is homogeneous and isotropic. A deeper idealization of the yarn was made by Zuo-Rong Chen and Ye,¹⁷ which treated the yarn as a bundle of elastic curved beams. In addition, the yarn was considered to have a cross section of elliptical shape and each fiber a circular cross section. They ignored the inter fiber friction between contacting fibers, which is valid when the surface of the fiber is very smooth, and when the yarn is lubricated by a liquid. Beard et al.¹⁸ also neglected the friction between fibers. Their model did not take into account any local or microscopic deformations, and they assumed the porous medium to be homogeneous and that the material response is described by the Hooke's Law.

Most assumptions are valid in some extent on synthetic fiber fabrics, but they are more questionable in plant fiber assemblies. Glass fibers assemblies are made of rovings with continuous and parallel fibers while plant fiber assemblies are made of yarns with discontinuous and twisted fibers (Fig. 2), thus the critical assumption of the fibers being uniformly packed used in many theoretical models is doubtful in plant fiber assemblies.¹⁹ The use of a unit cell that

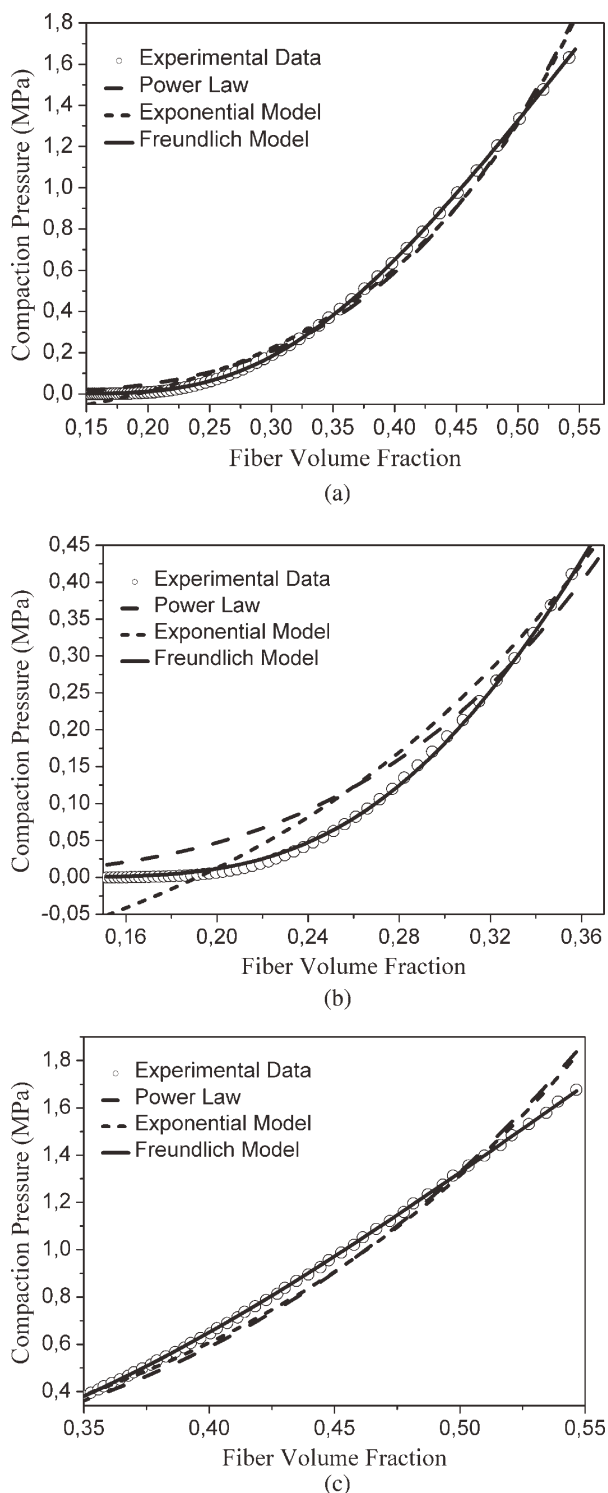


Figure 4 Dry tests Experimental compaction data fitted with three different empirical models. (a) Complete fiber content range, (b) low fiber content range, and (c) high fiber content range

repeats in the plane of the fabric is not possible due to the large variability in the surface density of natural fiber fabrics. Furthermore, natural fibers are hollow and the cell wall collapses when compressive forces are applied, and this permanent deformation

is not taken into account in synthetic fiber compaction models. In addition, this phenomenon causes a variation in the yarn cross-sectional area while it changes its shape. Neither the yarns nor the fibers can be treated as homogeneous or transversely isotropic solids due to the intrinsic anisotropy of plant fiber assemblies. Geometric assumptions are also questionable, because plant fiber cross section is not circular. Because of the natural fiber's rough surface morphology, the interfiber friction cannot be neglected. Figure 3 shows SEM images showing the smooth surface of glass fibers in contrast to the rough morphology of jute fibers. It can be seen that a single technical jute fiber is composed of several hollow elementary fibers, which are glued together in a matrix of lignin and hemicellulose.

Therefore, most of theoretical models found in literature are not applicable in natural fiber preforms, due to the very different fiber structure and assembly. The development of a theoretical model applicable to natural fibers is very complex and it would be valid only for the type of fiber and fabric that is being modeled, due to the intrinsic variability of plant fibers structure and composition depending on the origin and harvesting conditions. This matter may frustrate the effort needed to develop such models. Therefore, the use of empirical models is recommended, because they are easy to use and may characterize the compaction behavior of any natural fiber reinforcement effortlessly. However, it should be taken into account that the empirical parameters obtained with the model are valid only for the same type of fiber and fabric. In addition, fiber diameter, length, roughness, and cellulose content are strongly affected by soil and climate characteristics. Therefore, even if the reinforcement is provided by the same supplier and the cultivation technique remains the same, the fitting parameters of the compaction models are expected to change from one batch to another. Although it is not necessary to repeat all the experiments done in this work to choose the best model, a couple of routine compaction experiments should be conducted to obtain the new fitting parameters of the best-fitting-model, allowing to predict the compaction response of each batch of reinforcement. In a previous publication,³ it was found that the compaction behavior of fabrics taken from the same batch was very consistent, because when different tests were performed varying the final preform thickness, all the compaction curves superimposed in the shared fiber content range. Therefore, there is no need to perform a large number of tests and merge the experimental data in one single curve to determine the fitting parameters of the models.

A very simple model that can be used to fit most experimental data is the power law expression¹

TABLE I
Empirical Parameters of the Power Law

Power law model						
$\sigma(V_f) = A (V_f)^n$	<i>n</i> (dry test/wet test)			A (dry test/wet tests)		
Compaction Speed (mm/min)	First loading cycle	Second loading cycle	Third loading cycle	First loading cycle	Second loading cycle	Third loading cycle
0.5	3.83/4.36	5.81/5.03	6.69/5.24	19.75/31.23	55.2/31.96	87.48/35.54

TABLE II
Empirical Parameters of the Exponential Function

Exponential function			
$\sigma = Ae^{R_0 V_f} + y_0$	First loading cycle	Second loading cycle	Third loading cycle
Compaction Speed (mm/min)		<i>y</i> ₀ (dry test/wet test)	
	-0.2328/-0.1864	-0.0445/-0.0595	-0.0262/-0.051
		A (dry test/wet test)	
0.5	0.0719/0.0577	0.0032/0.0074	0.0064/0.0056
		<i>R</i> ₀ (dry test/wet test)	
	6.14/6.35	11.51/9.84	13.42/10.33

shown in eq. (1), where σ is the applied stress, V_f the volume fraction, and A and n are empirical parameters.

$$\sigma = A(V_f)^n \tag{1}$$

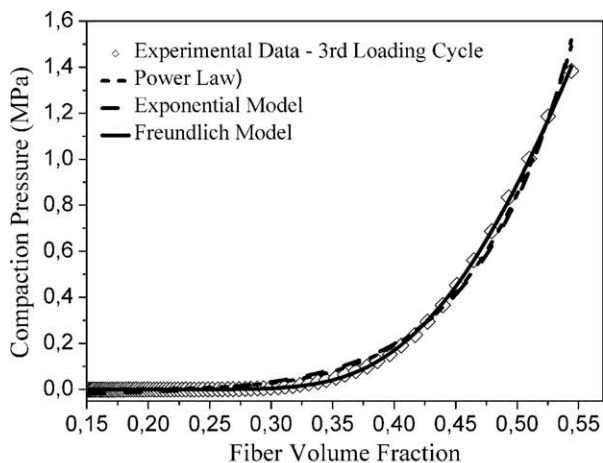
The exponential function shown in eq. (2) was also used in literature to fit the compaction curves. This function, which has three empirical constants A , R_0 , and y_0 , was used by Matsudaira and Qin to approximate the second part of the compression curve, while a linear equation was used to fit the first and third steps.²¹ They related the slope of the first linear regression with the bending of the fibers in the fabric surface and with the yarn structure, and the slope of the third linear regression with the fiber material transverse modulus. The parameter R_0 of the exponential function was related to the resistance to compression caused by interfiber friction.

$$\sigma = Ae^{R_0 V_f} + y_0 \tag{2}$$

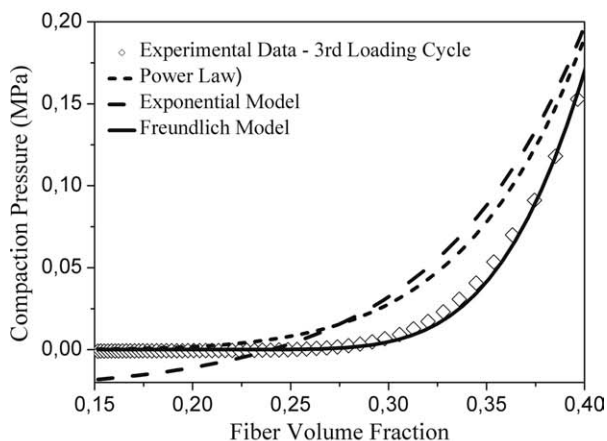
Some models were developed in literature for the relaxation process.^{1,18} Breard et al.¹⁸ proposed a simple model that takes into account the dual porosity structure of the fibrous medium. The model assumes that the material is linear viscoelastic. The dual porosity model distinguishes separately the viscoelastic effects of the macroscopic pores (i.e., gaps between yarns) and the microscopic pores (i.e., gaps between the fibers inside the yarns), and also the elastic component due to the intrinsic resistive characteristics of the solid phase material. These assumptions refer to pore size and thus the relaxation model would be applicable to woven natural fiber reinforcements, which present a dual porosity structure. However, they also considered that the fabrics were homogeneous and neglected the friction between fibers, and these assumptions are not applicable in plant fiber fabrics. Therefore, this model was used in this work as an empirical model, although it was developed theoretically. Equation (3) shows the solution of the differential

TABLE III
Empirical Parameters of the Freundlich Function

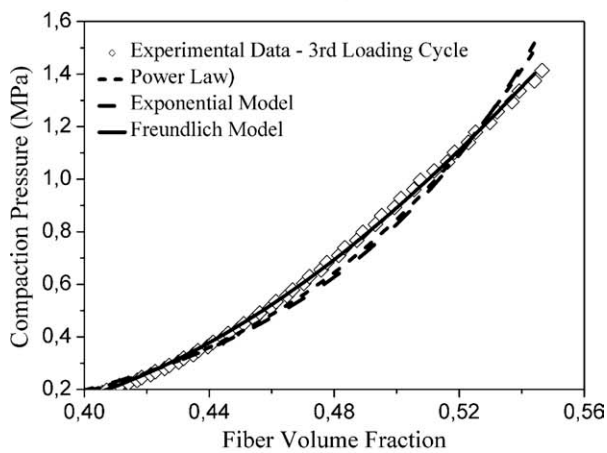
Freundlich function			
$\sigma(V_f) = a(V_f)^{b(V_f)-c}$	First loading cycle	Second loading cycle	Third loading cycle
Compaction Speed (mm/min)		<i>a</i> (dry test/wet test)	
	4.51095/4.394	5.4912/4.325	7.0656/4.551
		<i>b</i> (dry test/wet test)	
0.5	1.0083/1.123	0.8980/0.853	1.1431/0.902
		<i>c</i> (dry test/wet test)	
	0.8077/0.733	1.4273/1.296	1.386/1.297



(a)



(b)

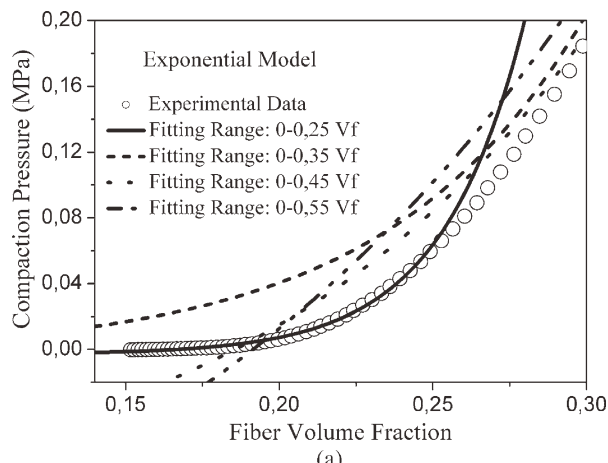


(c)

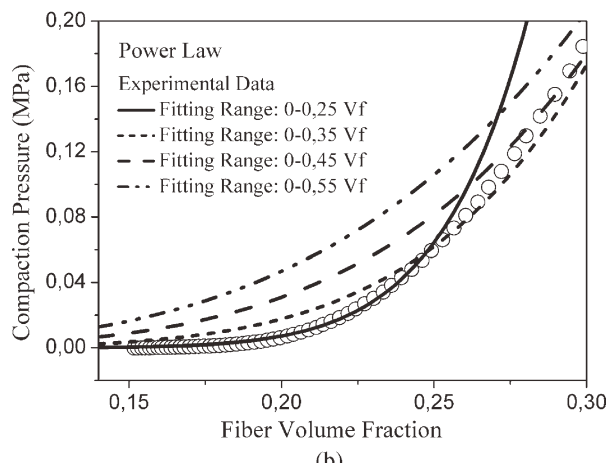
Figure 5 Fitting of the experimental data obtained at the third loading cycle of the dry tests. (a) Complete fiber content range, (b) low fiber content range, and (c) high fiber content range

equation governing the relaxation behavior in this model.

$$\sigma(t) = k_1 e^{-\frac{t}{\tau_1}} + k_2 e^{-\frac{t}{\tau_2}} + k_3. \quad (3)$$



(a)



(b)

Figure 6 The exponential model (a) and the power law (b) accuracy in the low pressures range improved as the data range considered in fitting the experimental data was reduced. The plots correspond to dry test experimental data

The two time constants τ_1 and τ_2 depend directly on the characteristics of the micro pores, the macro pores, and the solid phase material; K_1 and K_2 represent the

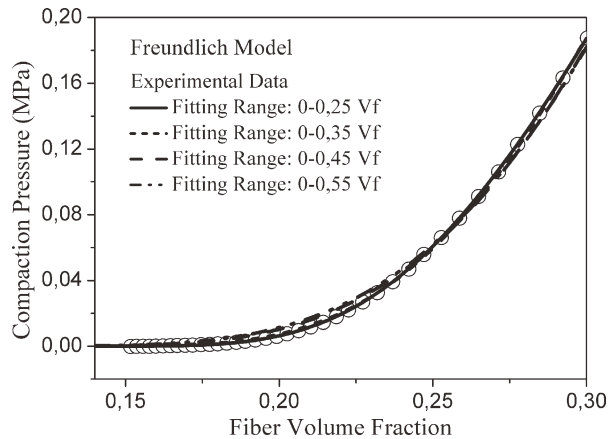
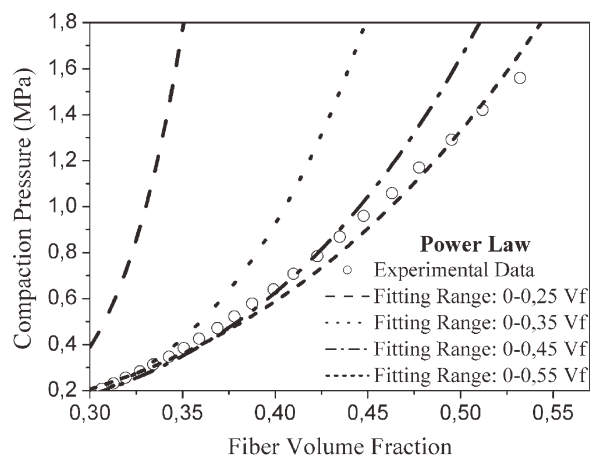
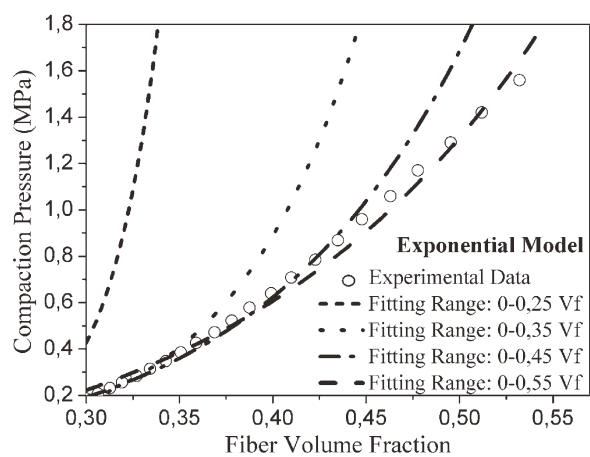


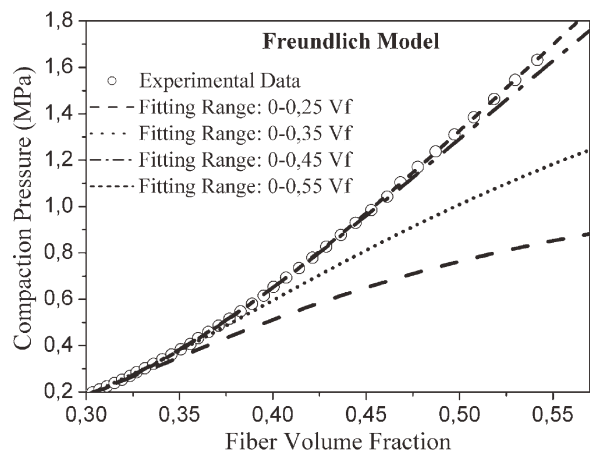
Figure 7 The Freundlich function obtained using all the experimental data fitted perfectly the low pressure part of the compaction curve. The plot corresponds to dry test experimental data



(a)



(b)



(c)

Figure 8 Extrapolation of the empirical models obtained in different data ranges (dry tests). (a) Power Law, (b) exponential function, and (c) Freundlich model

amplitudes of each contribution, and K_3 is the compaction pressure value after reaching a steady state.

COMPACTION EXPERIMENTS

An Instron 4467 Universal Testing Machine with a 30 KN load cell was used to carry out the compres-

sion tests. Circular preform samples (diameter = 0.13 m) were compressed at constant compaction rate, until the desired thickness or fiber volume fraction was achieved. These samples consisted of six layers of jute plain woven fabric (Castanhal Textil, Brasil; surface density = 300 g/m²). The fabrics were washed with a 2% V/V distilled water and detergent (15% active matter) solution, to remove contaminants and normalize the fabrics conditions for all the tests. Then, the fabrics were dried under vacuum at 60°C for 24 h. The compaction rate used was 0.5 mm/min, and the final thickness was chosen in order to obtain a fiber volume fraction of 0.55. The machine was programed to hold the final thickness for 10 min, whereas the load was recorded in order to analyze the stress relaxation in the preform. After the relaxation step, the compaction plate was removed at 50 mm/min until the initial thickness was reached, and then the test was repeated two more times. Thus, three loading cycles were obtained. It should be noticed that in most cases the preform thickness (or fiber volume fraction) after each loading cycle did not match the initial thickness (or unstressed fiber volume fraction), because the preforms experienced considerable permanent deformation.³ The wet compaction tests were carried out by compressing the preforms that had been placed inside a container filled with the test fluid: a 20% V/V water in glycerin (technical grade, Biopack, Argentina) solution. Such test fluid was chosen because its viscosity is close to typical infusion resin viscosity (0.2 Pa s).

Because of the great consistency found in the experimental work³ on the compaction behavior of the fabrics taken from the same batch, a single compaction curve was used to calculate the models' parameters for each experimental condition. The merge of experimental data of different tests carried out under the same conditions did not change significantly the value of the fitting parameters. Therefore, in order to keep the visualization of the curves clear, a single compaction curve was used and no error bars were

TABLE IV
Maximum Compaction Pressure Estimated with the Empirical Models

Maximum compaction pressure (MPa)			
Experimental value = 1.682 (at $V_f = 0.55$)			
Estimated with empirical models			
Fitting data range	Power law	Exponential	Freundlich
0–0.25 V_f	152.14 (8945%)	4723.3 (280713%)	0.852 (49.35%)
0–0.35 V_f	5.656 (236%)	9.757 (480%)	1.217 (27.65%)
0–0.45 V_f	2.652 (57.67%)	2.877 (71.05%)	1.661 (1.25%)
0–0.55 V_f	2.001 (18.97%)	1.876 (11.53%)	1.698 (0.95%)

TABLE V
Second-Order Exponential Model Parameters

Five Parameters Exponential Model (dry/wet)						
$\sigma(t) = k_1 e^{-\frac{t}{\tau_1}} + k_2 e^{-\frac{t}{\tau_2}} + k_3$						
Compaction speed (mm/min)	Final fiber volume fraction	k_3	k_1	τ_1	k_2	τ_2
0.5	0.35	0.75/0.59	0.12/0.15	228.7/20.66	0.11/0.23	16.78/284.65
	0.45	0.77	0.1	17.21	0.11	223.5
	0.55	0.81/0.7	0.09/0.11	227.3/21.94	0.08/0.17	18.5/289.87

added. However, it is highly recommended to perform a couple of compaction tests using the same experimental conditions in order to verify consistency among the curves. If significant discrepancies are found between them, it would be necessary to merge the experimental data in one single curve and fit the curve that includes all the data points, in order to obtain averaged values of the fitting parameters. In this work, a nonlinear least squares fitting procedure based on the Levenberg–Marquardt (LM) algorithm was used to calculate the fitting parameters of the models used.

RESULTS AND DISCUSSION

Modeling of the compaction step

Compaction pressure versus fiber volume fraction experimental data was fitted using the power law and the exponential function, being the two most used empirical models found in literature. Although both the models represented relatively well the compaction behavior of jute woven fabrics, the fitting was not perfect, as shown in Figure 4. The lack of accuracy of these models can be related to the fact that the compaction curve is composed of three different sections as was shown in Figure 1. De Jong et al.²² concluded in their work that it was impossible to represent the compaction curve with one single mathematical expression. The modeling of the three different sections of the curve separately can improve the experimental data fitting, but the ease of use of the model decreases substantially, because three different functions with their respective domains have to be defined. Therefore, a new model

was proposed, which fitted nearly perfect the experimental curve. The model is based on the Freundlich function and has three empirical parameters (a , b , c), as shown in eq. (4).

$$\sigma(V_f) = a(V_f)^{bV_f^c} \quad (4)$$

Tables I–III present the empirical parameters of these models for preforms compressed to 55% fiber content. The presence of the test fluid changes the value of the parameters but does not change the trend observed for the dry tests. The relationship between the empirical constants and aspects of fabric configuration such as weave pattern, number of layers, stacking method, shifting, and nesting is still uncertain.¹⁶ The values of n found in this work were consistent with the values presented in literature (3–11).²³

It can be seen in Figure 4 that all the proposed models fitted fairly well the experimental data. However, the Freundlich model was the most accurate one, representing almost exactly the compaction behavior of the fabrics. The accuracy of the models can be quantified by the value of the correlation coefficient R^2 , which was 0.9999 in the case of the Freundlich model, while in the case of the power law and exponential function was 0.9890 and 0.9910, respectively. In this case, the experimental data correspond to dry preforms compressed to a final fiber volume fraction of 0.55 at constant compression rate of 0.5 mm/min. The differences among the models can be seen with more detail in Figure 4(b,c), where the same curve plotted in Figure 4(a) was divided into a low and high fiber content curve.

TABLE VI
First-Order Exponential Model Parameters

Three Parameters Exponential Model (dry/wet)				
$\sigma(t) = Ae^{-\frac{t}{\tau}} + y_0$				
Compaction speed (mm/min)	Final fiber volume fraction	A	τ	y_0
0.5	0.35	0.151/0.267	118.66/158.75	0.767/0.62
	0.45	0.143	117.05	0.786
	0.55	0.121/0.197	118.95/151.77	0.826/0.727

TABLE VII
Power Law Relaxation Model Parameters

Power law model (dry/wet)			
$\sigma(t) = at^b$			
Compaction speed (mm/min)	Final fiber volume fraction	<i>a</i>	<i>b</i>
0.5	0.35	1.016/1.103	-0.0454/-0.0880
	0.45	1.020	-0.0421
	0.55	1.022/1.075	-0.0345/-0.0606

The applicability of the models used in this work on the second and third loading cycles was analyzed, because the shape of the compaction curves changed significantly after the first cycle. This analysis is shown in Figure 5 corresponding to the third loading cycle. If subsequent loading and unloading cycles are performed, the unstressed thickness of the preform decreases after each cycle, reaching a steady value after several tests.⁹ As a consequence, the load-displacement behavior changes from cycle to cycle, and the compaction stress needed to achieve a desired fiber volume fraction decreases as the number of cycles increases.²⁴ As the thickness of the sample is reduced due to permanent deformation, no resistance to compaction is observed until the compaction plate touches the sample. In addition, it can be seen that the first linear part of the curve is reduced after each loading cycle because the reduction of pores and gaps among the fibers have occurred in previous cycles. Therefore, the plots start almost at the second part of the curve related to the increase in the fiber to fiber contacts and interfiber friction. Although a slight decrease in the accuracy can be observed in the Freundlich model at the low fiber content range [Fig. 5(b)], the models behaved the same way as in the first loading cycle. Therefore, the same conclusions can be made. Apparently, the change in the compaction curve generated by the permanent deformation did not affect significantly the fitting accuracy of the models used in this work.

When fitting a compaction curve of an experiment conducted up to high fiber volume fractions (i.e., 55%) using the power law and exponential models, the fitting of the low fiber content part of the curve lacked accuracy, as shown in Figure 6. Therefore, in order to represent more exactly the compaction behavior at low compaction pressures, new empirical parameters should be determined based on data points within the desired fiber content range. On the other hand, the Freundlich function obtained by fitting all the experimental data up to the maximum fiber content (i.e., 55%) was found to fit perfectly the low fiber content range of the curve, as shown in Figure 7.

Sometimes it is impossible to obtain experimental curves at high fiber contents due to limitations in the load cell of the testing machine. This issue is frequent when compressing natural fiber fabrics due to the large inter fiber friction caused by the rough fiber morphology of plant fibers.¹⁹ However, the available clamping forces of the manufacturing equipment may be high enough to achieve such large fiber content. Therefore, the applicability of the empirical models beyond the maximum fiber content reached experimentally was studied. Figure 8 shows the experimental data fitted by the models, using different fiber volume fraction ranges. It can be seen that the proposed empirical models cannot be used to extrapolate the compaction behavior beyond the maximum fiber content reached in the compaction tests. However, the Freundlich model obtained by fitting the experimental data up to 45% of fiber content represented almost perfectly the whole compaction curve. On the other hand, the power law and the exponential function deviate from the experimental data quickly after the maximum fiber content considered was reached. Table IV shows the maximum compaction pressure values calculated with the three models using different fiber content fitting ranges. The relative error is shown between parentheses. It is clear that the Freundlich model is much better in predicting the maximum compaction pressure than the other models. The error obtained with this model fitted on experimental data below 25% fiber content was lower than the one obtained with the other models fitted in the range 0–0.45 of fiber volume fraction. It should be taken into account that the Freundlich model predicts a lower value than the real maximum compaction pressure while the other models predict a larger value. The results shows that if extrapolation further than the maximum fiber content reached in the tests is needed,

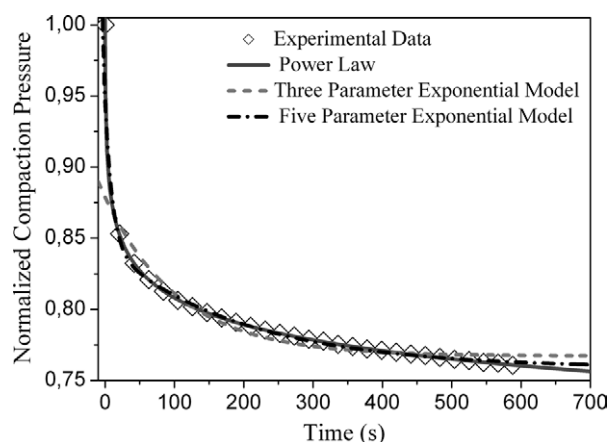


Figure 9 Empirical models used to represent the pressure relaxation process. The graph corresponds to preforms compressed to a final fiber volume fraction of 0.55

the model based on the Freundlich function should be used instead of the power law or exponential function.

Modeling of the relaxation stage

The second-order exponential model proposed by Breard et al.¹⁸ was found to fit almost perfectly the relaxation experimental data. However, the need of five constants is not practical for an empirical model. Therefore, the experimental data was fitted with other two empirical models based on less number of constants: a first-order exponential model and a power law model. The fitting parameters of these models are shown in Tables V–VII.

It was found that the first-order exponential model could not fit accurately the relaxation curve, while the power law model represented the relaxation behavior as good as the five parameters exponential model. Figure 9 shows the comparison between the three relaxation models.

CONCLUSIONS

Most of the assumptions used by the theoretical models developed in literature for fabrics made of synthetic fibers are not applicable in natural fiber fabrics. Therefore, these models should not be used to predict the compaction behavior of plant fiber fabrics. The development of a theoretical model valid on these types of reinforcements is very difficult, due to the complex structure of the fibers, the large variability on its properties, and the inhomogeneous nature of the fabrics made of natural fibers. Therefore, the use of empirical models is advised to represent the compaction response of natural fiber fabrics.

In this work, three empirical compaction models were considered. The most used empirical models in literature are the power law and the exponential function. They represented fairly well the compaction curve of jute fabrics, but the fitting was not perfect. These models are not capable of representing the compaction behavior with one single mathematical expression. The whole compaction curve can be fitted exactly by many power law or exponential functions valid in different pressure ranges, and this would increase the number of empirical constants needed. Therefore, a novel model based on the Freundlich function was proposed. This model fitted almost perfectly the whole compaction curve at all the pressure range. In addition, the applicability of the models beyond the maximum fiber content

reached experimentally was studied. It was found that, despite none of the models should be used to predict the compaction pressure at higher fiber contents than the experimentally reached, the Freundlich model led to a significantly smaller error than the other models.

The modeling of the relaxation stage was conducted by using three empirical models: a second-order exponential function, a first-order exponential function, and a power law. The latter has only two empirical constants and represented the relaxation as well as the five constants exponential model. The first-order exponential function, which has three empirical parameters, did not fit well the experimental data.

References

1. Kelly, P. A.; Umer R.; Bickerton S. *Composites Part A* 2006, 37, 868.
2. Francucci, G.; Rodriguez, E.; Vazquez, A. *Composites Part A* 2010, 41, 16.
3. Francucci, G.; Rodriguez, E.; Vazquez, A. *J Compos Mater*, 2011, in press.
4. Umer, R.; Bickerton, S.; Fernyhough, A. *Composites Part A* 2007, 38, 434.
5. Lundquist, L.; Willi, F.; Leterrier, Y.; Månson, J. A. E. *Polym Eng Sci* 2004, 44, 45.
6. Umer, R.; Bickerton, S.; Fernyhough, A. *Composites Part A* 2011, 42, 723.
7. Chen, B.; Chou T. W. *Compos Sci Technol* 1999, 59, 1519.
8. Potluri, P.; Sagar, T. V. *Compos Struct* 2008, 86, 177.
9. Chen, B.; Lang, E. J.; Chou, T. W. *Mater Sci Eng A* 2001, 317, 188.
10. Chen, B.; Cheng, A. H. D.; Chou, T. W. *Composites Part A* 2001, 32, 701.
11. Chen, B.; Chou, T.W. *Compos Sci Technol* 1999, 59, 1519.
12. Chen, B.; Chou, T. W. *Compos Sci Technol* 2000, 69, 2223.
13. Gutowski, T.G.; Cai, Z.; Bauer, S.; Boucher, D.; Kingery, J.; Wineman, S. *J Comput Math* 1987, 21, 650.
14. Toll, S. *Polym Eng Sci* 1998, 38, 1337.
15. Simáček, P.; Karbhari, V. M. *J Reinf Plast Compos* 1996, 15, 86.
16. Chen, Z. R.; Ye, L.; Kruckenberg, T. *Compos Sci Technol* 2006, 66, 3254.
17. Chen, Z. R.; Ye, L. *Compos Sci Technol* 2006, 66, 3263.
18. Breard, J.; Henzel, Y.; Trochu, F.; Gauvin, R. *Polym Compos* 2003, 24, 409.
19. Madsen, B. PhD Thesis, Technical university of Denmark, 2004.
20. Manfredi, L. B. PhD Thesis, Faculty of Engineering, UNMdP—INTEMA, 2000.
21. Matsudaira, M.; Qin, H. *J Text Inst* 1995, 86, 476.
22. De Jong, S.; Snaith, J. W.; Michie, N. A. *Text Res J* 1986, 57, 759.
23. Robitaille, F.; Gauvin, R. *Polym Compos* 1998, 19, 198.
24. Somashekar, A. A.; Bickerton, S.; Bhattacharyya, D. *Composites Part A* 2006, 37, 858.